International Journal on Artificial Intelligence Tools
Vol. 15, No. 3 (2006) 411–432

World Scientific
www.worldscientific.com

FEATURE EXTRACTION AND CLASSIFICATION OF FETAL HEART RATE USING WAVELET ANALYSIS AND SUPPORT VECTOR MACHINES

GEORGE GEORGOULAS*
Laboratory for Automation & Robotics, University of Patras, 26500, Patras, Greece
Tel.: +30 2610997293, Fax: +302610997309
georgoul@ ee.upatras.gr

CHRYSOSTOMOS STYLIOS
Department of Communications, Informatics and Management,
Technological Educational Institute of Epirus, Artas, Greece
Fax: +302610997309
stylios@teiep.gr

PETER GROUMPOS
Laboratory for Automation & Robotics, University of Patras, 26500, Patras, Greece
Tel.: +30 2610997295, Fax: +302610997309
groumpos@ee.upatras.gr

Since the fetus is not available for direct observations, only indirect information can guide the obstetrician in charge. Electronic Fetal Monitoring (EFM) is widely used for assessing fetal well being. EFM involves detection of the Fetal Heart Rate (FHR) signal and the Uterine Activity (UA) signal. The most serious fetal incident is the hypoxic injury leading to cerebral palsy or even death, which is a condition that must be predicted and avoided. This research work proposes a new integrated method for feature extraction and classification of the FHR signal able to associate FHR with umbilical artery pH values at delivery. The proposed method introduces the use of the Discrete Wavelet Transform (DWT) to extract time-scale dependent features of the FHR signal and the use of Support Vector Machines (SVMs) for the categorization. The proposed methodology is tested on a data set of intrapartum recordings were the FHR categories are associated with umbilical artery pH values, This proposed approach achieved high overall classification performance proving its merits.

Keywords: Discrete Wavelet Transform; Support Vector Machines; Fetal Heart Rate.

1. Introduction

Fetal Heart Rate (FHR) is the main indicator of fetal condition and, therefore, it is an indispensable means for both antepartum and intrapartum fetal surveillance. The FHR signal is obtained mainly through cardiotocography, also called Electronic Fetal Monitoring (EFM). EFM has become rapidly popular at least in North America and Western Europe, since fetal monitors became commercially available in the late 1960s

*Laboratory for Automation and Robotics, Department of Electrical and Computer Engineering, University of Patras, 26500 Rio Patras, Greece.

and early 1970s, as a result of the general belief that technology can resolve clinical problems.[1] In everyday clinical practice, FHR is displayed graphically on a printout and is manually interpreted by the clinician in charge depending on its visual aspect. More specifically the interpretation is performed following the guidelines given by the International Federation of Obstetrics and Gynaecology[2] (FIGO) and the National Institute of Health.[3] The major attractiveness for using EFM is the reassurance experienced by the obstetrician concerning the fetal condition as long as the FHR tracing is normal.

The instantaneous FHR (beats/min) during the intrapartum period, and after the rupture of the membranes, can be derived/acquired from the fetal electrocardiogram via scalp electrodes.[4] Even though there exist other non-invasive methods,[5] the use of scalp electrodes gives more reliable recordings.[6] The beat-to-beat variation of FHR reflects the time varying influence of the fetus' autonomic nervous system and its components[6] (sympathetic, parasympathetic branch) and, thus, it is an indicator of fetal well-being. Especially during the crucial period of labor, EFM is used as the main screening method of fetal acid base balance.[7]

Before the baby delivery, the exchange of oxygen and carbon dioxide by the fetus takes place within the placenta. If a pathological change occurs in either the maternal or fetal components of the placenta, this will interfere with placental-fetal gas exchange, causing fetal asphyxia or oxygen deficiency, with major health problems for the baby. If prolonged and/or profound, asphyxia can lead to fetal hypoxia, a condition in which blood supply to tissues is reduced. The redistribution of blood flow to oxygen-sensitive organs, such as the brain and heart, enables the fetus to survive short periods of oxygen deficiency. However, cerebral palsy or fetal death may occur if fetal hypoxia is sustained for prolonged periods. Asphyxia can lead to an accumulation of carbon dioxide in the blood and tissues resulting in fetal acidosis, a condition characterized by an increase in acidity reflected by a decrease in fetus' blood pH. Due to the fact that cerebral palsy is often diagnosed several years after birth, the objective of inspecting FHR patterns is not to detect which babies will have cerebral palsy, but to detect those that are at significant high risk so as to warn the obstetrician and allow intervention before there is irreversible damage. Thus, it is of great importance to be able to associate FHR traces with umbilical artery pH values.

The significance of FHR interpretation many researchers to investigate FHR signal processing. The Dublin randomized trial has revealed an increase in operative vaginal deliveries in patients monitored using EFM during the intrapartum period.[8] In addition, studies of FHR reliability have shown significant inter-observer and intra-observer variation in tracing interpretation.[9] This inconsistency in interpretation and the increase of false positive diagnoses guided the introduction of computerized systems for the analysis and interpretation of FHR. New approaches for FHR processing are based on the technological advances in computers, along with new signal processing methods. These types of methods and systems range from simple feature extraction[10-17] to sophisticated classification programs.[18-27] Some approaches have shown promising results but none has achieved broad acceptance and there is still room for improvement.

The goal of finding prognosis methods to deliver healthy babies with minimal intervention to the mother will remain a challenge for some time.

Since the FHR signal conveys much more information than what is usually interpreted by doctors,[26] in this research work we investigate new methods based on advanced signal processing and innovative feature extraction methods that will provide indices of fetal condition. We propose for the first time an integrated method to discriminate fetuses suspicious of developing metabolic acidosis, using Discrete Wavelet Transform (DWT) for the extraction of time-scale features and Support Vector Machines (SVMs) for the classification task.

Wavelets are a novel tool, different from the traditional Fourier analysis in the way they localize information in the time-frequency plane. In particular, they are capable of trading one type of resolution for the other, which makes them especially suitable for the analysis of non-stationary signals. As a result, they have been employed in many applications in biomedical signal processing.[28, 29] The most appealing feature of wavelets is that they can decompose a signal into a number of scales, each scale representing a particular "coarseness" of the signal under study.[30] They have already been used successfully for the analysis of the inter-beat intervals of adult hearts.[31, 32] There have also been some initial attempts to use wavelets for the analysis of FHR during the second stage of labor.[26, 33] Most of these approaches, however, do not use any of the time domain information included in the wavelet coefficients and presume that the signal under investigation is stationary.

SVMs have recently been developed in the framework of statistical learning theory[34] and have proved highly successful in a number of applications both for nonlinear regression and pattern classification.[35, 36] SVMs have the ability to generalize well on unknown data without requiring problem-domain knowledge, which makes them very appealing for pattern recognition involving difficult real life problems.[35, 37, 38]

This paper is structured as follows: In section 2 a brief mathematical introduction is given including the background of DWT and SVMs. Section 3 presents the proposed integrated method for FHR signal preprocessing (noise-artifact removal, segmentation) and then the FHR feature extraction and classification. Section 4 discusses the experimental results of applying the proposed methodology to a data set. Finally section 5 concludes the paper, comparing the proposed methods with other approaches and suggesting future directions.

2. Mathematical Background

2.1. *Wavelets*

Similar to most physiological signals, FHR is a non-stationary signal, where the main non-stationarities are the baseline and the acceleration/deceleration events.[13] Therefore, traditional Fourier analysis is not suitable for this particular type of signal, unless it is restricted to sufficient short segments. On the other hand, wavelets are a relatively new very powerful mathematical tool for signal processing that have been successfully used

in a number of biomedical applications.[28, 29] In plain language, a wavelet is a short-term duration wave.

The wavelet transform of a time signal is an expansion of the signal in terms of a family of functions, which are localized in both time and frequency domains and are generated from a single function called the mother wavelet $\psi(t)$, by "dilation" and by "translation".

$$\psi_{a,b}(t) = \frac{1}{\sqrt{a}}\psi\left(\frac{t-b}{a}\right), \tag{1}$$

where $a \in \mathbb{R}^+, b \in \mathbb{R}$. For most practical applications on measured data, the wavelet dilation and translation parameters a, b are restricted only to discrete values leading to Eq. (2).

$$\psi_{m,n}(t) = \frac{1}{\sqrt{a_0^m}}\psi\left(\frac{t - nb_0a_0^m}{a_0^m}\right). \tag{2}$$

For practical purposes, the simplest and most efficient discretization comes by choosing $a_0 = 2$ and $b_0 = 1$ (dyadic grid arrangement or dyadic lattice).

$$\psi_{m,n}(t) = \frac{1}{\sqrt{2^m}}\psi\left(\frac{t-n2^m}{2^m}\right) = 2^{-m/2}\psi\left(2^{-m}t - n\right), \tag{3}$$

where $(m,n) \in \mathbb{Z}^2$. The translation parameter determines the location of the wavelet in the time domain, while the dilation parameter determines its location in the frequency domain as well as the scale or extent of the time frequency localization.

Any signal may be decomposed into its contributions in different regions of the time-frequency domain (time-scale) by projecting it onto the corresponding basis functions. Therefore, for a continuous signal, the wavelet coefficients, the time-scale representation of a continuous signal $x(t)$, are given by the dyadic wavelet transform, resulting in wavelets coefficients.

$$T_{m,n} = \int_{-\infty}^{\infty} x(t)\psi_{m,n}^*(t)dt, \tag{4}$$

which measures the "similarity" between the signal and the basis function. If the discrete dyadic grid wavelets are chosen to be orthogonal, the information stored in a wavelet coefficient $T_{m,n}$ is not repeated elsewhere. Therefore, the information represented at a certain scale m is disjoint from the information at all other scales. Smaller scales correspond to higher frequency components (speaking in Fourier terms). Moreover, each wavelet coefficient encompasses information not only concerning the scale but also the time (window) that "produced" this information.

For a discrete signal $x[i]$, i=0,...,$M-1$ and for a real wavelet the coefficients are given by Eq. (5).

$$T_{m,n} = 2^{-m/2}\sum_{i=0}^{M-1} x[i]\psi\left(2^{-m}i - n\right). \tag{5}$$

Obviously, different mother wavelets give birth to different classes of wavelets, and hence the behavior of the decomposed signal can be quite different. However, according

to Thuner[30] in their work involving the analysis of heartbeat intervals, the obtained results were similar when experimenting with different types of mother wavelets. In this work, we experimented with a variety of mother wavelets in order to identify the best one for each of the specific implementations.

The wavelets that we employed were proposed by Daubechies[39] and they have the appealing property of having compact support and the wavelet transform can be computed with finite impulse response conjugate mirror filters using a fast filter bank algorithm. We experimented using Daubechies, Symmlets and Coiflets families, with different number of vanishing moments. Wavelets with p vanishing moments can suppress parts of signals, which are polynomials up to degree $p-1$. Daubechies wavelets have a support of minimum size for any given number p of vanishing moments. Symmlets are also wavelets of minimum support, for any given number p of vanishing moments, but they are more symmetric compared to Daubechies. Coiflets, which are also nearly symmetrical, do not have minimum support but their scaling and wavelet function have the same number of vanishing moments. In Fig. 1 a mother wavelet for each one of the three families is depicted.

For more information, the interested reader can refer to one of the excellent books that can be found in the literature.[39, 40]

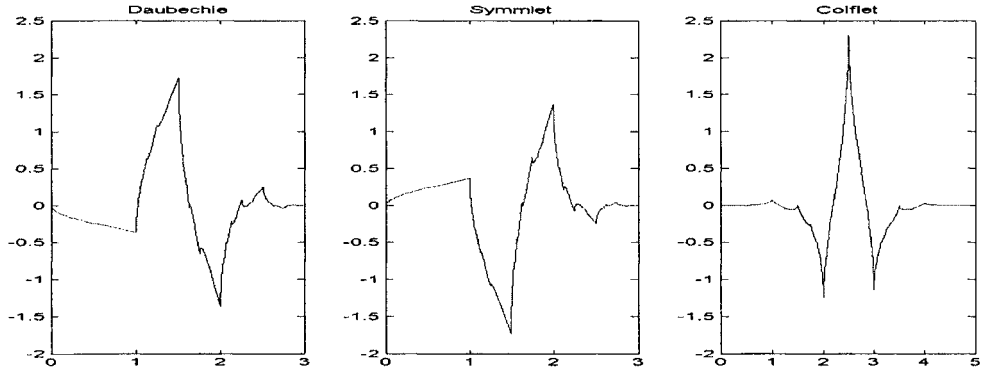

Fig. 1. Three mother wavelets with two vanishing moments.

2.2. *Support Vector Machines*

Support Vector Machines (SVMs) are a new family of learning machines,[34] which have been successfully used for a variety of pattern classification tasks.[36] The main idea behind SVMs, when dealing with a pattern classification problem, is to find an "optimal" hyperplane as the solution to the learning problem. By the term "optimal", it is suggested that for a separable classification task, the hyperplane $(\mathbf{w},b)$ with the maximum margin or distance from the closest data points belonging to the different classes is selected.

Formally speaking, having a set of points that each belongs to one of two classes, for a binary classification or dichotomization problem, i.e. a training set $\{\mathbf{x}_i, y_i\}$, $i = 1,...,n$, where each point $\mathbf{x}_i$ is a d-dimensional vector, and $y_i \in \{-1,1\}$ is a label that specifies to which one of the classes the point $\mathbf{x}_i$ belongs, and if the two classes are linearly separable, then there exists at least one hyperplane $(\mathbf{w},b)$ which can perfectly separate the positive from the negative examples. The hyperplane that maximizes the margin of separation is the one for which the Euclidian norm of the weight vector $\|\mathbf{w}\|^2$ is minimum and at the same time satisfies the constraints of Eq. (6).

$$y_i\left(\mathbf{w}^T\mathbf{x}_i + b\right) - 1 \geq 0 \quad \forall i\,. \tag{6}$$

This is a classical quadratic optimization problem with inequality constraints that can be solved using Lagrange multipliers. However, in real life problems the different classes are not linearly separable. Therefore, two actions usually need to be performed:

- nonlinear mapping of the input space into a potential much higher feature space,
- construction of an optimal hyperplane, allowing for some misclassifications.

The nonlinear mapping is performed because according to Cover's theorem[41]: "A complex pattern-classification problem cast in a high-dimensional space is more likely to be linearly separable than in a low-dimensional space".

Therefore, for every vector $\mathbf{x}_i$ we calculate a vector $\boldsymbol{\varphi}(\mathbf{x}) = \left[\phi_1(\mathbf{x}), \phi_2(\mathbf{x}), ...\phi_f(\mathbf{x})\right]^T$ corresponding to a nonlinear mapping from $\mathbb{R}^d$ to the higher dimensional space $\mathbb{R}^f$ $(f > d)$.

The optimal hyperplane is found as the solution to the minimization problem of Eq. (7).

$$\text{Minimize} \quad \frac{1}{2}\mathbf{w}^T\mathbf{w} + C\sum_{i=1}^{n}\xi_i\,, \tag{7}$$

$$\text{subject to} \quad y_i\left(\mathbf{w}^T\boldsymbol{\varphi}(\mathbf{x}_i) + b\right) \geq 1 - \xi_i \quad \text{and} \quad \xi_i \geq 0 \quad \forall i\,, \tag{8}$$

where the ξ_i are called slack variables that measure the deviation of a data point from the ideal condition of pattern separability, and C is a positive user specified parameter that penalizes margin errors, i.e. patterns that lie within the margin as well as those that are on the wrong side of the decision surface.

The solution for this optimization problem of Eq. (7), subject to the constraints Eq. (8), is given by the solution of the primal Lagrangian Eq. (9).

$$L_p(\mathbf{w},b,\boldsymbol{\xi},\boldsymbol{\alpha},\boldsymbol{\beta}) = \frac{1}{2}\mathbf{w}^T\mathbf{w} + C\sum_{i=1}^{n}\xi_i - \sum_{i=1}^{n}\beta_i\xi_i - \sum_{i=1}^{n}a_i\left(y_i\left(\mathbf{w}^T\boldsymbol{\varphi}(\mathbf{x}_i) + b\right) - 1 + \xi_i\right), \tag{9}$$

which, in turn, leads to the dual maximization problem of the dual Lagrangian Eq. (10).

$$L_d(\boldsymbol{\alpha}) = \sum_{i=1}^{n}a_i - \frac{1}{2}\sum_{i,j=1}^{n}a_i a_j y_i y_j\left(\boldsymbol{\varphi}^T(\mathbf{x}_i)\boldsymbol{\varphi}(\mathbf{x}_j)\right), \tag{10}$$

subject to the constraints of Eq (11).

$$\sum_{i=1}^{n} a_i y_i = 0 \text{ and } 0 \le a_i \le C \quad \forall i . \tag{11}$$

The solution of the above optimization problem leads to the "optimal" discriminating function of Eq (12).

$$f(\mathbf{x}) = sign\left(\sum_{i=1}^{n} y_i a_i \left(\varphi^T(\mathbf{x}_i)\varphi(\mathbf{x}) \right) + b \right). \tag{12}$$

The points for which $a_i > 0$ are called Support Vectors and they are usually a small portion of the original data set.

The inner product in the feature space can be written in the form of Eq (13).

$$\varphi^T(\mathbf{x}_i)\varphi(\mathbf{x}_j) = K(\mathbf{x}_i, \mathbf{x}_j), \tag{13}$$

where K is called the inner-product kernel. A kernel function is a function in input space and, therefore, we do not explicitly perform the nonlinear mapping $\varphi(\cdot)$. Instead of calculating the inner product in a feature space $\varphi^T(\mathbf{x}_i)\varphi(\mathbf{x}_j)$, one can indirectly calculate it using the kernel function $K(\mathbf{x}_i, \mathbf{x}_j)$. Therefore, by selecting an appropriate symmetric positive semi-definite kernel function, it is not necessary to know what the actual mapping is.[36] Different kernels produce different learning machines and different discriminating hypersurfaces.

The above formulation of SVM is inappropriate in case of imbalanced distributions and a different approach is needed. This is a very common situation when dealing with medical data and the SVM algorithm has to be adapted. The proposed approach is to use different regularization (also addressed as penalty) parameters C^+ and C^- so as to penalize more heavily the undesired type of error, and/or the errors related to the class with the smallest population.[42, 43] Therefore, for this case, the optimization problem is modified as shown by Eq. (14).

$$\text{Minimize} \frac{1}{2}\mathbf{w}^T\mathbf{w} + C^- \sum_{i:y_i=-1}^{n} \xi_i + C^+ \sum_{i:y_i=+1}^{n} \xi_i , \tag{14}$$

$$\text{subject to } y_i\left(\mathbf{w}^T\varphi(\mathbf{x}_i) + b\right) \ge 1 - \xi_i \text{ and } \xi_i \ge 0 \quad \forall i . \tag{15}$$

Choosing higher penalty value for the class with the smallest population (which in most cases happens to be the class that needs to be correctly identified) results in a bias for larger multipliers a_i for that class. This induces a decision boundary, which is more distant from that class.

3. New Integrated FHR Feature Extraction and Classification Methodology

The proposed overall procedure for processing Fetal Heart Rate (FHR) signal, feature extraction using DWT and classification using SVM is depicted in Fig. 2. The novelty and core of the proposed method is the feature extraction stage using wavelet analysis (third block) as well as the classification stage employing SVMs. Wavelets are introduced for the transformation of FHR into wavelet coefficients (using different mother wavelets), different sets of which are tested using different configurations of the SVM classifier. This proposed procedure is the outcome of an extensive investigation in the field of FHR processing.

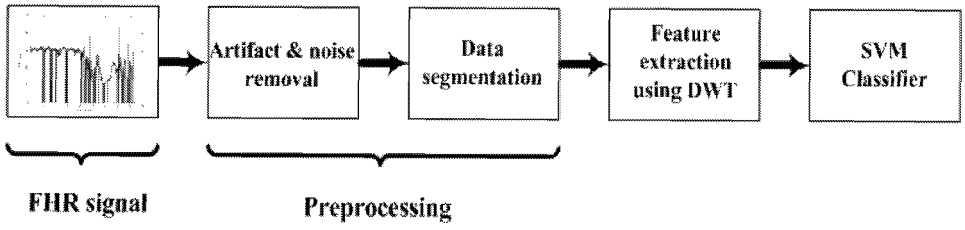

Fig. 2. The block diagram of the proposed methodology.

3.1. *Artifact and noise removal*

FHR is a very noisy signal with a lot of spiky artifacts and even periods of missing data due to the movement of the baby and the stress induced during the labor.

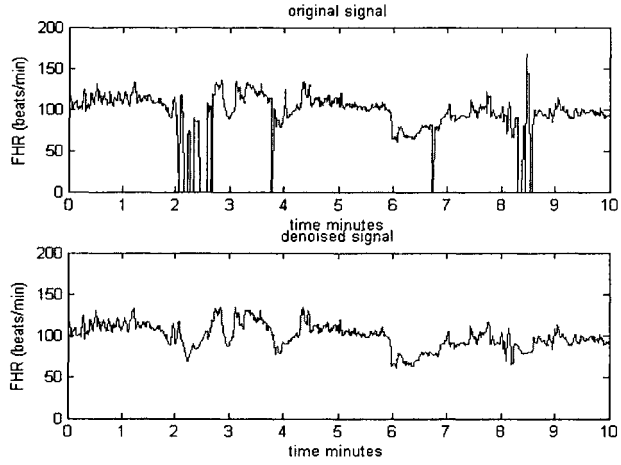

Fig. 3. a) Initially acquired FHR signal, b) signal after the removal of artifacts.

This kind of noise cannot be eliminated in the source and it is always present in any cardiotocographic record. It is reported that missing data in fetal heartbeats records can amount to about 20-40% of total data.[33] Therefore, the first stage in the proposed methodology involves the implementation of an algorithm to eliminate this kind of noise from the FHR signal (Fig. 3), which was first proposed by Bernardes.[44]

3.2. *Data segmentation*

The proposed method investigates whether FHR traces can be used to foresee the level of the umbilical artery pH at delivery. Even thought metabolic acidosis is not a sudden state into which the fetus falls, FHR recordings corresponding to the final minutes before the delivery can more reliably be correlated with pH measurements. Thus, in this work we focused on the last 5-10 minutes of the recordings, those that are closer to delivery and we applied the proposed method to segments with time duration of 5 and 10 minutes. These segments were taken as close as possible to the end of the recording. It must be mentioned that in some of the recordings the final 1-2 minutes had to be excluded because the FHR signal was totally obscured by noise.

3.3. *Feature extraction stage via wavelet transform*

The third stage of the proposed methodology consists of two actions performed on the FHR signal: (a) transformation of FHR into a set of wavelet coefficients and (b) feature extraction based on those coefficients. The FHR signal for the corresponding time segment is transformed using discrete wavelet transform up to scale $m=5$ using Eq. (5) (Fig. 4). As mentioned in section 2.1, different mother wavelets have been tested (Daubechies, Symmlets and Coiflets) leading to different representations.

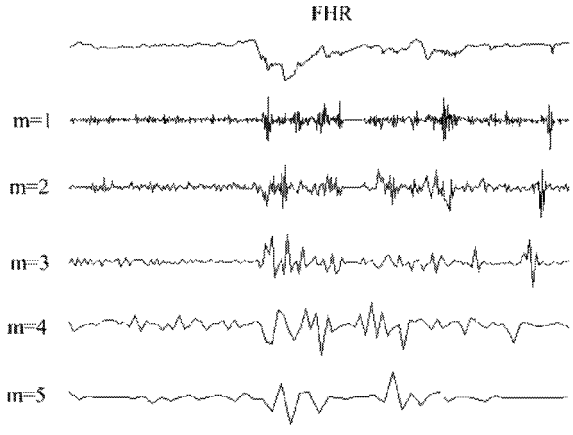

Fig. 4. The initial FHR signal on the upper part and its decomposition to wavelet coefficients for scales m=1,2,3,4,5.

The feature extraction part operates on the wavelet coefficients at different scales. Wavelets have the ability to represent deterministic features using a small number of relatively large coefficients, while stochastic processes contribute to all the coefficients and are approximately decorrelated. If a wavelet decomposition results in a few large coefficients, then those coefficients can represent the whole signal, neglecting the rest of the coefficients, with a low error. As a result, these coefficients can give valuable information for classification.[45] Therefore, what is needed is to find a function to describe the concentration of coefficients. The most common measure is the Shannon entropy. Shannon entropy for a discrete distribution p_i, $i = 1,2,...,N$ is given by Eq. (16).

$$S = -\sum_{i=1}^{N} p_i \log(p_i) \text{ with } \sum_{i=1}^{N} p_i = 1 \text{ and } p_i \log(p_i) = 0, \text{ if } p_i = 0. \tag{16}$$

The maximum entropy possible from a distribution occurs when the information is evenly spread across the signal. The more clustered the distribution, the lower the entropy. In the case of a signal the minimum entropy occurs when all the information is contained in a single location. Therefore the Shannon entropy is a measure of impurity within a set of instances and it can be extended to the normalized wavelet coefficient energies to find those sets of coefficients that contain the most information. Fig. 5 illustrates three cases of signals with maximum, intermediate and minimum entropy. The signal that has only one value different from the other nine, is the most "impure" signal and has the minimum entropy, while the signal that has all its values equal to 0.1 is the one with the maximum entropy.

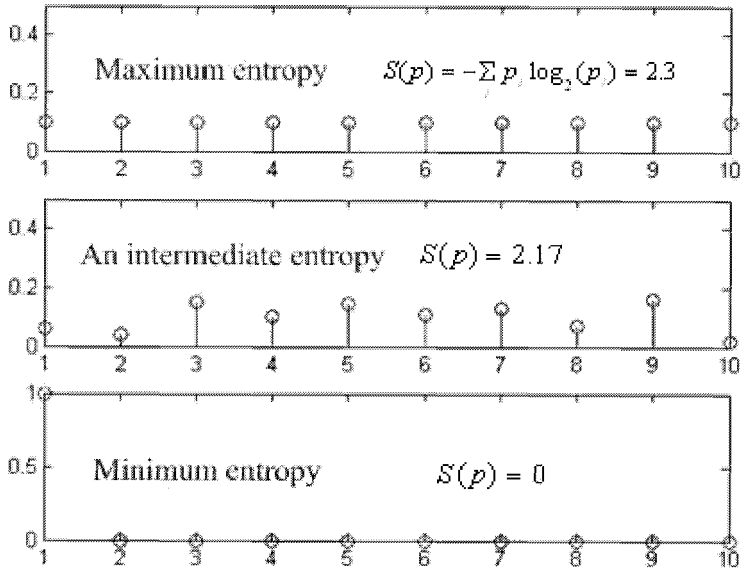

Fig. 5. Three cases of signals representing maximum, intermediate and minimum entropy.

3.3.1. *Feature sets selection*

An important stage is the selection of the most suitable feature set and for this reason we examined four feature sets for two different signal durations 5 and 10 minutes in order to test these sets and determine the most suitable.

Feature set 1:
For scales $m=2$ to $m=4$ we measured the absolute value of the wavelet coefficients for each one of the three scales and we used the coefficient with the highest absolute value, along with its index (providing information about its occurrence) as features to be fed to the SVM classifier. For example, at scale m:

$$f_{m,1} = sign\left(T_{m,n}\right) \cdot \max\left(\left|T_{m,n}\right|\right) \text{ for } n = 1,\ldots,N_m, \tag{17}$$

where N_m is the number of wavelet coefficients at scale m and:

$$f_{m,2} = \arg\max_{n}\left(\left|T_{m,n}\right|\right) \text{ for } n = 1,\ldots,N_m. \tag{18}$$

Thus, for each FHR segment, the feature set includes six features:
Fset1: $\{ f_{2,1}, f_{2,2}, f_{3,1}, f_{3,2}, f_{4,1}, f_{4,2} \}$.

Feature set 2:
Moving one scale "up", we repeated the aforementioned procedure using the scales $m=2$ to $m=5$, which leads to a new set of eight features:
Fset2: $\{ f_{2,1}, f_{2,2}, f_{3,1}, f_{3,2}, f_{4,1}, f_{4,2}, f_{5,1}, f_{5,2} \}$.

Feature set 3:
For scales $m=2$ to $m=4$ we introduced a sliding window and for the normalized energies of the wavelet coefficients inside this window, we calculated the Shannon entropy seeking for the location of the window that minimizes that quantity (Fig. 6). The minimum calculated entropy, along with the location of the window for which this happens -the centre of the window- are selected as features that we introduced to characterize each scale. The length of the window was adapted according to the number of coefficients at each scale –it was reduced by a factor of two as we were moving from scale m to scale $m+1$. The normalization of the energies was performed with respect to the coefficients at that specific scale. For example, at scale m we calculated:

$$S(i) = -\sum_{j=0}^{W_m-1} \frac{\left(T_{m,i+j}\right)^2}{\sum_{j=0}^{W_m-1}\left(T_{m,i+j}\right)^2} \log \frac{\left(T_{m,i+j}\right)^2}{\sum_{j=0}^{W_m-1}\left(T_{m,i+j}\right)^2} \text{ for } i = 1,\ldots,N_m - W_m + 1, \tag{19}$$

where W_m is the length of the sliding window at scale m.

$$f_{m,3} = \min\left(S(i)\right) \text{ for } i = 1,\ldots,N_m - W_m + 1, \tag{20}$$

$$\text{and } f_{m,4} = \arg\min_i\left(S(i)\right) - 1 + \frac{W_m}{2} \text{ for } n = 1,\ldots N_m. \tag{21}$$

Thus, for each FHR segment we calculated a total of six features:
Fset3: $\{ f_{2,3}, f_{2,4}, f_{3,3}, f_{3,4}, f_{4,3}, f_{4,4} \}$.

Feature set 4:
Again moving one scale "up" we repeated the procedure described in the selection of feature set 3 using the scales $m=2$ to $m=5$, leading to a feature vector with eight features:
Fset4: $\{ f_{2,3}, f_{2,4}, f_{3,3}, f_{3,4}, f_{4,3}, f_{4,4}, f_{5,3}, f_{5,4} \}$.

The coefficients from scale $m=1$ were excluded from this feature extraction stage because they corresponded to the high frequency components and, thus, they were considered as representations of the "noise" content of the signal.

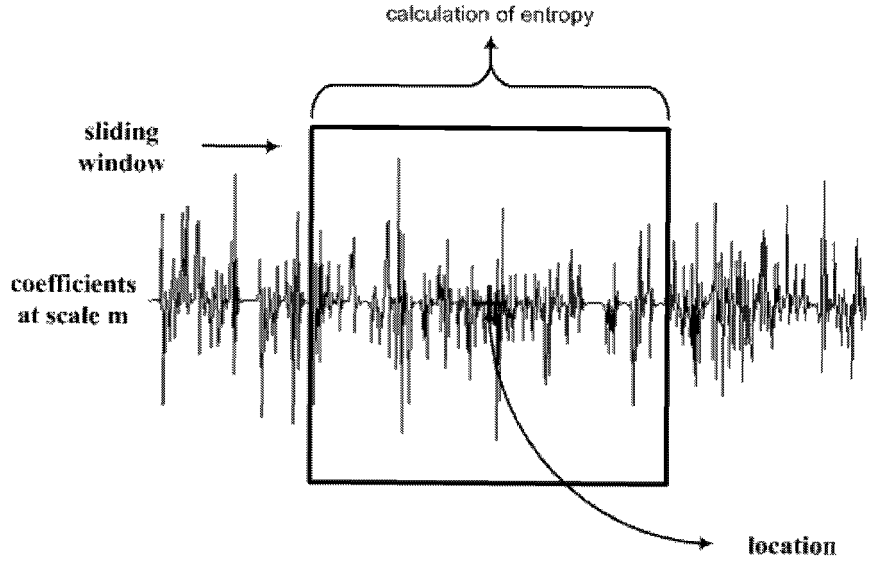

Fig. 6. Feature extraction using a sliding window for finding window with the minimum entropy.

3.4. *Classification stage*

The classification stage involves the employment of a SVM and follows the feature extraction stage. It is well known that in the case of SVMs, the classification depends on how the inner-product kernel is generated; so different learning machines can be constructed with quite different nonlinear decision surfaces.[38, 41] In this work, we propose the use of RBF kernels for SVMs because they proved to give better results.[46] Fig. 7,

illustrates a SVM, where the hidden layer has as many nodes as the number of support vectors found during the training process. For the RBF kernel, each one of the support vectors is the centre of the Gaussian bump:

$$K(\mathbf{x},\mathbf{x}_i)=\exp\left(-\frac{1}{2\sigma^2}\|\mathbf{x}-\mathbf{x}_i\|^2\right), \tag{22}$$

where the width σ is specified *a priori* by the user and it is common for all the kernels.

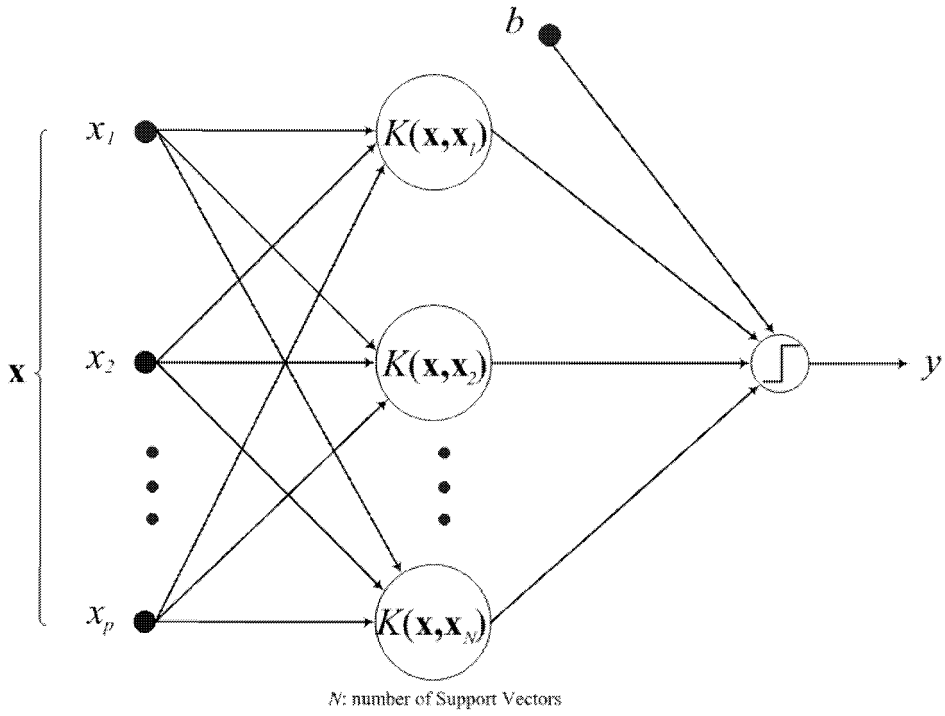

Fig. 7. A graphical representation of a Support Vector Machine Classifier.

The imbalanced nature of the problem made even more difficult the classification stage and prompted us to adopt the modified SVM scheme with the two penalty parameters C^+ and C^-. It has been reported[47-49] and proved through our exhaustive experimentation that the ratio C^+/C^- should be set to the inverse of the corresponding cardinalities of the classes. Therefore, keeping their ratio C^+/C^- constantly equal to three and using different values for the values C^+ and C^-, we experimented with different values of the width parameter σ. This was performed in a systematic manner (a simple grid search) covering a variety of values for both the two adjustable parameters.

4. Experimental Tests and Results

The proposed methodology (Fig. 2) was implemented and applied to a data set consisting of 80 signals, which had been acquired using scalp electrodes. The data set involved fetuses that had either umbilical artery pH less than 7.1 (20 cases) or higher than 7.2 (60 cases). Newborns with umbilical artery pH in the range (7.1, 7.2) were not included in the data set. Signals that belonged to fetuses with umbilical artery blood pH less than 7.1 corresponded to the group of cases that were "at risk". Fetuses with umbilical arterial blood pH higher than 7.2, formed the "normal" group. It must be mentioned that different thresholds settings can be found in the literature.[6]

All FHR records had been acquired during the final stage of labor and, in fact, as close as possible to delivery. This means that the data sets were free of time-bias and hopefully a direct association can be made between the segment of the signal used and the newborn's blood pH. The recordings had durations ranging from 20 minutes to more than 1 hour.

Because of the quite small number of labeled data, in order to test the performance of our methodology, we employed 10-fold cross-validation.[41] We divided the 80 cases into 10 (non-overlapping) subsets; each one consisting of six examples from the "normal" and two from the "at risk" group. The SVM classifier was trained using all subsets except for one, and the validation error was assessed by testing the subset left out. We repeated this procedure 10 times, each time using a different subset for testing and we averaged the performance over the 10 experiments. In order to compare the efficiency of the proposed method, we also tested three conventional classifiers: the Nearest Neighbor (NNC), the Linear (LC) and the Quadratic (QC) classifiers using the same four feature sets for the two different time duration segments (5 and 10 minutes).

Following the medical terminology, we refer to the babies with umbilical artery pH value less than 7.1 as the positive cases (the cases that *are* "at risk") and the babies with pH higher than 7.2 as the negative cases (the cases that *are not* "at risk" -the "normal" group).

	Predicted Negative	**Predicted Positive**
Actual Negative	**TN**	**FP**
Actual Positive	**FN**	**TP**

Fig. 8. Confusion Matrix.

The performance of a classification process can be described by a confusion matrix, like the one illustrated in Fig. 8. In the confusion matrix (Fig. 8), *TN* is the number of negative examples correctly classified (True Negatives), *FP* is the number of negative examples incorrectly classified as positive (False Positives), *FN* is the number of positive examples incorrectly classified as negative (False Negatives) and *TP* is the number of positive examples correctly classified (True Positives).

In problems with imbalanced data, accuracy $a=(TP+TN)/(TP+FP+TN+FN)$ is probably not the best measure to evaluate performance. A more appropriate metric, proposed by Kubat,[51] is the geometric mean:

$$g=\sqrt{a^{+}\cdot a^{-}}, \tag{23}$$

where $a^{+}=TP/(TP+FN)$ is the accuracy observed separately on positive examples (also known with the term sensitivity) and $a^{-}=TN/(FP+TN)$ is the accuracy observed separately on negative examples (also known with the term specificity).

When the feature sets *Fset1* and *Fset2* were used, extracted from 5 minute time segments, didn't yield satisfactory results. Both the conventional classifiers and the SVM achieved low performance, as shown on Table 1 and Table 2. The high accuracy of the quadratic classifier is superficial since it manages only to classify correctly the cases with the high pH. On the other hand, as in all experiments the SVM classifier manages to have a balanced performance.

Table 1. Classification results for *Fset1* extracted from 5 minute segments.

	NNC	LC	QC	SVM
a	72.5	76.25	82.5	72.5
a^{+}	40	5	50	80
a^{-}	83.33	100	93.33	70
g	57.73	22.36	68.3	74.83

Table 2. Classification results for *Fset2* extracted from 5 minute segments.

	NNC	LC	QC	SVM
a	67.5	76.25	73.75	75
a^{+}	30	10	86.67	70
a^{-}	80	98.33	35	76.67
g	48.99	31.36	55.08	73.26

It is apparent from Table 3 and Table 4 that *Fset3* and *Fset4* extracted from 5 minute time segments gave better results. Both the conventional classifiers and the SVM have the ability to satisfactory identify the normal cases for feature sets *Fset2* and *Fset3*. Additionally, the SVM clearly outperforms the conventional classifiers concerning the classification of the "at risk" cases. Daubecies wavelets with 11 vanishing moments seem to be the best choice for the analyzing wavelet for these particular feature sets, even though high performance has also been achieved with Symmlets and Coiflets.

Table 3. Classification results for *Fset3* extracted from 5 minute segments.

	NNC	LC	QC	SVM
a	72.5	83.75	63.75	86.25
a^+	40	45	40	70
a^-	83.33	96.67	71.67	91.67
g	59.44	65.96	53.54	80.1

Table 4. Classification results for *Fset4* extracted from 5 minute segments.

	NNC	LC	QC	SVM
a	82.5	82.5	85	88.75
a^+	55	55	60	75
a^-	91.67	91.67	93.33	93.33
g	71	71	74.8	83.67

The next set of experiments examined the four feature sets extracted from 10 minute segments. As in the case of 5 minute segments, *Fset1* and *Fset2* didn't yield satisfactory results. In fact the results were quite similar for both time segments.

Table 5. Classification results for *Fset1* extracted from 10 minute segments.

	NNC	LC	QC	SVM
a	72.5	76.25	65	70
a^+	50	5	30	80
a^-	80	100	76.67	66.67
g	63.25	22.36	47.96	73.03

Table 6. Classification results for *Fset2* extracted from 10 minute segments.

	NNC	LC	QC	SVM
a	75	76.25	71.25	67.5
a^+	45	10	40	85
a^-	85	98.33	81.67	61.67
g	61.85	31.36	57.16	72.4

Table 7. Classification results for *Fset3* extracted from 10 minute segments.

	NNC	LC	QC	SVM
a	78.75	77.5	75	80.25
a^+	50	40	35	70
a^-	88.33	90	88.33	85
g	66.46	60	55.6	77.14

Table 8. Classification results for *Fset4* extracted from 10 minute segments.

	NNC	LC	QC	SVM
a	81.25	82.5	82.5	88.75
a^+	55	55	45	70
a^-	90	91.67	95	95
g	70.36	71	65.38	81.55

It is shown in Table 7 and Table 8 that *Fset3* and *Fset4* for 10 minute segments perform very well. This was also the case of the 5 minute segments. The additional information, when coefficients from scale $m=5$ are included, improves the performance, not only of the SVM classifier but also of the conventional classifiers.

Comparing and examining the results presented in Tables 1-8, it has to be mentioned that if someone looks only the overall accuracy then he would mistakenly conclude that the employed conventional classifiers perform in a similar manner compared to the SVM classifier. However, this is not the case. A more reliable comparison of the different classification methods has to involve the investigation of the 5th row of the tables, which depicts the geometric mean for each classifier. Under this prism, the SVM classifier in every case outperforms the conventional classifiers.

As it can be concluded from Tables 1, 2, 5 and 6, the isolated coefficients (*Fset1* and *Fset2)* didn't yield satisfactory results. However, it must be mentioned that isolated coefficients were examined because this application of the wavelet transform has been used successfully in EEG analysis[51] and driven by that we decided to experiment with these coefficients too. It seems that the underlying physiology of the FHR signal cannot be represented by this oversimplified approach. On the other hand, the features (*Fset3* and *Fset4)* based on the entropy measure seem to be able to reflect fetal condition in terms of the umbilical artery pH value in a much more accurate way. This is justified in Tables 3, 4, 7 and 8 by the high performance of all classification approaches involved.

Moreover, the inclusion of features from scale $m=5$ improves the performance. Therefore, the best feature set for the particular problem of the association of FHR with umbilical artery pH is *Fset4*.

5. Conclusions

In this work, a novel integrated and automated methodology was proposed and used for the first time for the feature extraction and classification of FHR signal. The novelties of this methodology are: the introduction of wavelets to extract time scale dependent features, the extensive examination and selection of feature sets and, the use of SVM for the classification task. The overall procedure proved that the use of time-scale dependent features yields high classification performance for both classes ("at risk" and "normal"). The results are more satisfactory compared to other previous works involving the same data set, where features extracted from time and frequency domain, along with morphological features were used.[46]

Due to the special design of this methodology, no direct comparison can be made with other approaches.[22, 25] Chung and his group[22] achieved accuracy of 77% (sensitivity of 87.5% and specificity of 75%) using a pH value equal to 7.15 as the borderline between normal and abnormal cases. In one of our experiments and for 5 minute segments and *Fset4* (extracted using Daubechies wavelets with 11 vanishing moments) we had accuracy of 83.8% (sensitivity of 80% and specificity of 85%). That can be regarded as comparable to the results reported in[22] (these results were not tabulated in Table 4 since the geometric mean (82.46%) was not the best achieved). Concerning the work of Salamalekis[25], where a threshold of pH equal to 7.10 is used, higher sensitivity (100%) but lower specificity (86.2%) compared to our results (sensitivity of 75%, specificity of 93.3%) is reported. What is also interesting is that their results were achieved using Daubechies wavelets with 10 vanishing moments, which is close to the wavelets that gave the best results in our case. Due to the fact that apart from the FHR signal, measurements of functional oxygen saturation of fetal arterial blood were used in that work, no direct comparison can be made.

According to the National Institute of Health[3] one research recommendation is to investigate the correlation of FHR patterns with immediate outcome measures of asphyxia, such as blood gases and acid-base state (in particular acidosis). Starting from this point, we proposed and examined a method to associate FHR features to low umbilical pH value, which can be regarded as a meaningful clinical outcome. Furthermore, someone could argue regarding the choice of the threshold for the pH value, that this perhaps should be lower for the "at risk'' set, but since there is no consensus concerning that, we chose a threshold for the "at risk" group on the limit of normality.[6] The limit chosen to characterize the "at risk" cases is lower than those used in Refs. 22 and 52 where it was chosen equal to 7.15.

The proposed methodology is automated, which means that no intervention or input from the obstetricians is required. However, if we want to put this method into service, we have to test it for a large number of cases, through rigorous validation and verification to ascertain the stability and generalization of the proposed method. At this point we are only able to state that the results are very promising. It also needs to be mentioned that there are no commercially available computer systems that make interpretations concerning the period of labor.[53] Another outcome that we demonstrated in this work is that the final minutes of labor are correlated with the umbilical artery pH of the newborn, something which was viewed with skepticism in the early 90s.[54]

In conclusion, we must mention that the presented methodology seems to perform very well in our experiments, but some of its aspects need to be addressed in the future. In this research work, we used a predefined time segment in order to apply our methodology for the discrimination between the two classes and we did not investigate whether we can find the "line" at which the fetus is moving from a normal state to a "risky" one. However the onset of a situation that could compromise the fetus is of paramount importance for clinical practice and towards this direction we will focus on in future work. Furthermore, in this work we didn't incorporate in our analysis the information conveyed by the signal reflecting the Uterine Activity (UA), which is also

provided my cardiotocographs. In future research we are going to develop a computerized system –part of it will be a module for the FHR analysis-, which will serve as a complementary tool in University Hospital, Obstetrics and Gynecology department.

Acknowledgments

Authors would like to thank Prof. João Bernardes, Department of Gynecology and Obstetrics, Porto Faculty of Medicine, Porto, Portugal for advising us in medical related issues and his useful comments and suggestions in writing this paper. In addition to this, Prof. J. Bernardes provided us with the fetal heart rate data collected within the Research Project POSI/CPS/40153/2001, from Fundação para a Ciência e Tecnologia, Portugal.

References

1. C. B. Martin, Electronic fetal monitoring: a brief summary of its development, problems and prospects, *Eur. J. Obstet. Gynecol. Repr. Biol.* **78**(2) (1998) 133-140.
2. G. Rooth, A. Huch and H. Hough, Guidelines for the use of fetal monitoring, *Int. J. Gynecol. Obstet.* **25** (1987) 159-167.
3. National Institute of Child Health and Human Development Research Planning Workshop, Electronic fetal heart rate monitoring: Research guidelines for interpretation, *Am. J. Obstet Gynecol.* **177** (1997) 1385-1390.
4. C. M. Carter, Present-day performance qualities of cardiotocographs, *Br. J. Obstet. Gynaecol.* **100**(Suppl. 9) (1993) 10-14.
5. M. Peters, J. Crowe, J. F. Pieri, H. Quartero, B. Hayes-Gill, D. James, J. Stinstra and S. Shakespeare, Monitoring the fetal heart non-invasively: A review of methods, *J. Perinat. Med.* **29**(5) (2001) 408-416.
6. J. T. Parer and W. B. Saunders *Handbook of fetal heart rate monitoring*, 2nd edn (W. B Saunders Company, Philadelphia Pennsylvania, 1997)
7. H. P. van-Geijn, Developments in CTG analysis, *Bailliers Clin. Obstet. Gynaecol.* **10**(2) (1996) 185-209.
8. D. MacDonald, A. Grant, M. Sheridan-Pereira, P. Boylan and I. Chalmers, The Dublin randomized controlled trial of intrapartum fetal heart rate monitoring, *Am. J. Obstet Gynecol.* **152**(5) (1985) 524-539.
9. J. Bernardes, A. Costa-Pereira, D. Ayres-de-Campos, H. P. van-Geijn and L.Pereira-Leite, Evaluation of interobserver agreement of cardiotocograms, *Int. J. Gynaecol. Obst.* **57**(1) 1997 33-37.
10. D. Arduini, G. Rizzo, G. Piana, A. Bonalumi, P. Brambilla and C. Romanini, Computerized Analysis of Fetal Heart Rate: I. Description of the System (2CTG), *J. Maternal Fetal Invest.* **3** (1991) 159-163.
11. R. Mantel, H. P. Van-Geijn, F. J. M. Caron, J. M. Swartjes, E. E. van-Woerden and H. W. Jongsma, Computer analysis of antepartum fetal heart rate: 1. Baseline Determination, *Int. J. Biomed. Comput.* **25**(4) 1990 261-272.
12. R. Mantel, H. P. van-Geijn, F. J. M. Caron, J. M. Swartjes, E. E. van-Woerden and H. W. Jongsma, Computer analysis of antepartum fetal heart rate: 2. Detection of accelerations and decelerations, *Int. J. Biomed. Comput.* **25**(4) 1990 273-286.

13. J. Jezewski, K. Horoba, A. Gacek, J. Wrobel, A. Matonia and T. Kupka, Analysis of nonstationarities in fetal heart rate signal, Inconsistency measures of baselines using acceleration/deceleration patterns, in *Proc. 7th ISSPA* (France, Paris 2003) 34-38.
14. K. Maeda, Computerized analysis of cardiotocograms and fetal movements, *Bailliers Clin. Obstet. Gynaecol.* **4**(4) (1990) 1797-1813.
15. M. Mongelli, R. Dawkins, T. Chung, D. Sahota, J. A. Spenser and A. M. Chang, Computerised estimation of the baseline fetal heart rate in labour: the low frequency line, *Br. J. Obstet. Gynaecol.* **104**(10) (1997) 1128-1133.
16. G. M. Taylor, G. J. Mires, E. W. Abel, S. Tsantis, T. Farrell, P. F. W. Chien and Y. Liu, The development and validation of an algorithm for real time computerized fetal heart rate monitoring in labour, *Br. J. Obstet. Gynaecol.* **107**(9) (2000) 1130-1137.
17. C. Ulbricht, G. Dorffner and A. Lee, Neural Network for recognizing patterns in cardiotocograms, *Artif. Intell. Med.* **12**(3) (1998) 271-284.
18. B. Guijarro-Berdinas, A. Alonso-Betanzos and O. Fontenla-Romero, Intelligent analysis and pattern recognition in cardiotocographic signals using a tightly coupled hybrid system, *Artificial Intelligence* **136**(1) (2002) 1-27.
19. D. Ayres-de-Campos, J. Bernardes, A. Garrido, J. Marques-de-Sa and L. Pereira-Leite, SisPorto 2.0 – a program for automated analysis of cardiotocograms, *J. Matern. Fetal Med.* **9**(5) (2000) 311-318.
20. G. Magenes, M. G. Signorini and D. Arduini, Classification of cardiotocographic records by neural networks, in *Proc. IJCNN* **3**(3) (2000) 3637-3641.
21. S. Cazares, L. Tarassenko, L. Impey, M. Moulder and C. W. G. Redman, Automated identification of abnormal cardiotocograms using neural network visualization techniques, in *Proc. 23rd Annual International Conference of the IEEE* **2** (2001) 1629-1632.
22. T. K. H. Chung, M. P. Mohajer, X. J. Yang, A. M. Z. Chang and D. S. Sahota, The prediction of fetal acidosis at birth by computerized analysis of intrapartum cardiotocography, *Br. J. Obstet. Gynaecol.* **102** (1995) 454-460.
23. G. S. Dawes, M. Moulden and C. W. Redman, Computerized analysis of antepartum fetal heart rate, *Amer. J. Obstet. Gynecol.* **173**(4) (1995) 1353-1354.
24. W. Krause, A computer aided monitoring system for supervision of labour, in Computers in perinatal medicine, ed. K. Maeda (Elsevier Science, Amsterdam, 1990), 103-111.
25. E. Salamalekis, P. Thomopoulos, D. Giannaris, I. Salloum, G. Vasios, A. Prentza and D. Koutsouris, Computerised intrapartum diagnosis of fetal hypoxia based on fetal heart rate monitoring and fetal pulse oximetry recordings utilising wavelet analysis and neural networks, *Br. J. Obstet. Gynaecol.* **109**(10) 2002 1137-1142.
26. M. G. Signorini, G. Magenes, S. Cerutti and D. Arduini, Linear and nonlinear parameters for the analysis of fetal heart rate signal from cardiotocographic recordings, *IEEE Trans. Biomed. Eng.* **50**(3) (2003) 365 – 374.
27. J. F. Skinner, J. M. Garibaldi and E. C. Ifeachor, A Fuzzy System for Fetal Heart Rate Assessment, in *Proc. 6th Fuzzy Days Conference*, (Gernamny, Dortmund, 1999) 20-29.
28. M. Unser and A. Aldrubi, A Review of Wavelets in Biomedical Applications, in *Proc. IEEE* **84**(4) (1996) pp 626-638.
29. A. Aldrubi and M. Unser, *Wavelets in medicine and biology*, (CRC Press, 1996).

30. S. Mallat, A theory for multiresolution signal decomposition: the wavelet representation, *IEEE Trans. Patt. Anal. Machine Intell.* **11**(7) (1989) 674-793.
31. S. Thuner, M. C Feurstein. and M.C Teich, Multiresolution wavelet analysis of heartbeat intervals discriminates healthy patients from those with cardiac pathology, *Phys. Rev. Lett.* **80**(7) (1998) 1544-1547.
32. P. C. Ivanov, M. G. Rosenblum, C. K. Peng, J Mietus, S. Havlin, H. E. Stanley and A. L. Goldberger, Scaling behaviour of heartbeat intervals obtained by wavelet-based time series analysis, *Nature* **383** (1996) 323-327.
33. Z. R. Struzik and W. J. V. Wijngaarden, Cumulative effective Hölder exponent based indicator for real time fetal heartbeat analysis during labour, Report INS-R0110 (2001).
34. V. Vapnik, *Statistical Learning Theory*, (Wiley, New York, 1998).
35. K. R. Muller, S. Mika, G. Ratsch, K. Tsuda and, B. Scholkopf, An Introduction to Kernel-Based Learning Algorithms, *IEEE Trans.Neur. Networks* **12(2)** (2001) 181-201.
36. C. J. C. Burges, A Tutorial on Support Vector Machines for Pattern Recognition, *Data Mining and Knowledge Dicovery* **2**(2) (1998) 121-167.
37. K. Veropoulos, Cristianini and C. Campbell, The Application of Support Vector Machines to Medical Decision Support: A Case Study, in *Proc. ECCAI Advanced Course in Artificial Intelligence* (1999).
38. J. Shawe-Taylor and N. Cristianini, *Kernel Methods for Pattern Analysis* (Cambridge University Press, 2004).
39. I. Daubechies, *Ten Lectures on wavelets* (SIAM, Philadelphia, 1992).
40. S. Mallat, *A Wavelet Tour of Signal Processing* (Academic Press, 1999).
41. S. Haykin, *Neural Networks: A Comprehensive Foundation*, 2nd edn. (Prentice Hall, New Jersey, 1999).
42. E. Osuna, R. Freund and F. Girosi, Support Vector Machines: Training and applications, MIT A. I. Lab., A. I. Memo AIM-1602 (1997).
43. K. Veropoulos, C. Cambell and N. Cristianini, Controlling the sensitivity of support machines, in *Proc. Int. Joint Conf. AI* (Sweden, Stockholm, 1999).
44. J. Bernardes, C. Moura, J. Marques-de-Sa and L. Pereira-Leite, The Porto system for automated cardiotocographic signal analysis, *J. Perinat. Med.* **19**(1-2) (1991) 61-65.
45. H. Zhang, Ho, T. B. & Lin, M. S. A Non-Parametric Wavelet Feature Extractor for Time-Series Classification, in *Proc. 8th Pacific-Asia Conf. Knowledge Discovery Data Engineering (PAKDD)*, eds. H. Dai, R. Srikant, C. Zhang (Australia, Sydney, 2004), 595-603.
46. G. Georgoulas, C. Stylios and P. Groumpos, A Novel methodology for Fetal Heart Rate Signal Classification During the Intrapartum Period, *IEEE Trans. Biomed. Eng.* **33,** (5) (2006).
47. R. Akbani, S. Kwek and N. Japkowicz, Applying Support Vector Machines to Imbalanced Datasets, in *Proc. 15th Eur. Con. Machine Learning (ECML'2004)*, eds. J.-F. Boulicaut, F. Esposito, F. Giannotti and D Pedreschi (Italy, Pisa, 2004).
48. K. K. Lee, S. R. Gunn, C. J. Harris and P. A. S. Reed, Classification of Imbalanced Data with Transparent Kernels, in *Proc. INNS-IEEE Int. Joint Conf. Neural Networks*, (U.S.A., Washington DC, 2001), 2410-2415.
49. S. Perkins, N. R. Harvey, S. P. Brumby and K. Lacker, Support Vector Machines for Broad Area Feature Extraction in Remotely Sensed Images, in *Proc. SPIE 4381*, (2001), 286-295.

50. M. Kubat and S. Matwin, Addressing the Curse of Imbalanced Data Sets: One-Sided Selection, in *Proc. 14th Int. Conf. Machine Learning* , (1997), 179-186.
51. N. Hazarika, J. Z. Chen, A. C. Tsoi and A. Sergejew, Classification of EEG signals using the wavelet transform, *Signal Processing* **59** (1997) 61-72.
52. R. K. Strachan, D. S. Sahota, W. J. V. Wijngaardenc, D. K. Jamesa and A. M. Z. Chang, Computerised analysis of the fetal heart rate and relation to acidaemia at delivery, *Int. J. Obstet. Gynaecol.* **108**(8) (2001) 848-852.
53. Society of Obstetricians and Gynecologists of Canada, Fetal Health Surveillance in Labour (Part II), *J. Obstet. Gynaecol. Canada*, (112) (2002) 1-7.
54. G. S. Dawes, Computerized fetal heart rate analysis, in *A critical appraisal of fetal surveillance*, eds. H. P. van-Geijn and F. J. A, Copray (Elsevier Science, Amsterdam, 1994), 311-314.